General Disclaimer

One or more of the Following Statements may affect this Document

- This document has been reproduced from the best copy furnished by the organizational source. It is being released in the interest of making available as much information as possible.

- This document may contain data, which exceeds the sheet parameters. It was furnished in this condition by the organizational source and is the best copy available.

- This document may contain tone-on-tone or color graphs, charts and/or pictures, which have been reproduced in black and white.

- This document is paginated as submitted by the original source.

- Portions of this document are not fully legible due to the historical nature of some of the material. However, it is the best reproduction available from the original submission.

Produced by the NASA Center for Aerospace Information (CASI)

Kazuhisa Miyoshi and Donald H. Buckley
Lewis Research Center
Cleveland, Ohio

NASA

PLASTIC DEFORMATION AND WEAR PROCESS AT A SURFACE
DURING UNLUBRICATED SLIDING[†]

by Takashi Yamamoto[*] and Donald H. Buckley

National Aeronautics and Space Administration
Lewis Research Center
Cleveland, Ohio

ABSTRACT

The plastic deformation and wear of a 304 stainless steel surface sliding against a aluminum oxide rider with a spherical surface (the radius of curvature: 1.3 cm) were observed by using scanning electron and optical microscopes. Experiments were conducted in a vacuum of 10^{-6} Pa and in an environment of 5×10^{-4} Pa of chlorine gas at 25° C. The load was 500 grams and the sliding velocity was 0.5 centimeter per second. The deformed surface layer which accumulates and develops successively is left behind the rider, and step-shaped proturbances are developed even after single pass sliding under both environmental conditions. A fully developed surface layer is gradually torn off leaving a characteristic pattern. The mechanism for tearing away of the surface layer from the contact area and sliding track contour is explained assuming the simplified process of material removal based on the adhesion theory for the wear of materials.

INTRODUCTION

The friction behavior of solid materials can be understood on the basis of several principal concepts of tribological surface properties which include thin surface films and real contact area. These concepts frame the so-called adhesion theory of friction. Accurate observations of the wear process lead

---

[†]Some of the material presented herein is contained in NASA TP-2036 and TP-2037, 1982.

[*]Tokyo University of Agriculture and Technology, Tokyo, Japan, and National Research Council - NASA Research Associate.

to the conclusion that material transfer occurs during unlubricated sliding contact for metals; and, that in certain cases, it is in fact even observed under the condition of lubricated sliding contact. For the wear mechanism based on adhesion, however, a critical counterargument has been frequently offered, which is that the material transfer does not necessarily guarantee the formation of wear fragments unless the fracture or detachment occurs subsequently at or in the contact location. Therefore, the subject is still greatly debated particularly with respect to how wear fragments are produced in the process of relative motion between contacting surfaces.

In the case of a soft rider for example, sliding on a hard material larger in size, the surface layer of the soft rider will probably transfer to the mating harder material in the manner of tearing off and smearing. The weight of the rider generally successively decreases with sliding distance for this type combination. The process of losing the soft material is, therefore defined reasonably as wear. Based on morphology, the wear process may be substantially the same as for erosion in the sense that a material transfer phenomenon results in a decrease of weight of the rider. The wear process or material transfer mechanism however, for the combination of a hard rider sliding on a soft material is considerably different and more difficult to define. The plastic deformation caused by the action of the leading edge of the rider in this latter case has been studied by many investigators in relation to abrasive wear and grinding processes (refs. 1 to 4). If the grit or rider has the proper geometrical shape, a wear fragment will be produced in the microcutting process or in the final process in plowing, independent of the definition of wear and its relation to metal transfer (ref. 1). For contacts with well-finished surfaces, however, the inclination angle or slope for practical topography is generally small. A majority of rake angle effects may

2

exist in the range of the values under which plowing prevails. In such configurations, the deformation occurring in the contact area should be restricted by the mating material. In other words, the surface layer cannot deform as freely as in the process involving individual grits or asperities. Therefore, the microcutting process cannot be applied directly to the wear mechanism for this kind of contact.

The adhesive wear theory does not as yet offer a suitable mechanism for wear fragment formation because proponents of the theory have a tendency to discuss it from an atomistic viewpoint. In most practical problems, contact occurs over a finite area that is larger than the atomic scale. Therefore, a good deal of knowledge is needed for larger contact areas as well as atomic size contact.

The following mechanisms are considered as relatively comprehensive and overcome the vulnerablity of the adhesive wear mechanism. Landheer and Zaat offered a simplified mechanism for the development of junction and metal transfer applicable to practical configurations (ref. 5).

Antler and Cocks also observed deformation behavior for the transferred material, wedge formation between sliding surfaces using several combinations of material, and suggested wear mechanisms for their experimental results (refs. 6 to 11). Sasada, et al., offered a mechanism that involves incipient wear fragment formation based on the measurement of variations in the gap between sliding surfaces using similar configurations (ref. 12). These studies indicate one distinct process in which wear fragments can be produced. The detachment process based on the adhesion theory, however, of wear fragment formation has not as yet been discussed satisfactorily.

One of the present authors has indicated with many combinations of solid-to-solid contacts under simplified conditions that an interfacial adhesion

3

bond which occurs between the contacting surfaces is generally stronger than the cohesive bond in the cohesively weaker of the two materials and that the cohesively weaker metal generally transfers to the cohesively stronger on separation of the surfaces (ref. 13). There remains unresolved, however, the problem of the fracture process with respect to how the surface layer of the soft material is separated from the bulk material in the contact area region. The present objective is to establish the "boundary conditions" for large scale contact and to determine how the fundamental information obtained at the atomic scale can be applied to larger scale engineering surfaces. Such investigation should assess the morphological behavior of the contact region. In this paper therefore, observations of plastic deformation occurring under ordinary sliding contact using scanning electron and optical microscopy are described from a morphological point of view. The wear mechanism and deformation behavior are discussed on the basis of the boundary conditions to which a realistic wear mechanism should be subject incorporating the fundamentals of adhesion.

EXPERIMENTAL APPARATUS AND PROCEDURE

Apparatus

The experiments were conducted in a vacuum chamber (fig. 1). The vacuum system was pumped by sorption pumps and an ion pump. Pressure in the vacuum system was read with an ion gage. The specimens consisted of a disk 6.5 centimeters in diameter and 1.3 centimeters thick and a roller-shaped rider with a spherical surface 2.5 centimeters in radius. The specimens are shown in the apparatus schematic in figure 1. The disk specimen was mounted on a drive shaft that was rotated by means of a magnetic drive assembly. The drive assembly provides for rotation in the range of zero to 15 mm/sec speeds. The roller can be rotated with the friction force between the roller and the

4

disk. In this study, the rotation of the roller was held up by a stopper. Therefore, pure sliding was conducted at the contact surface.

The friction force working between the disk and the rider was continuously recorded during the experiment. The beam containing the rider specimen was welded in a bellows assembly that was gimbal mounted to the vacuum system. The gimbal mounting permits deadweight loading of the rider against the disk surface. The beam containing the rider can move in two directions in the horizontal plane at right angles to the deadweight loading. As the disk rotated movement of the rider was restricted by a cable attached to a temperature-compensated strain gage. These gages measured the friction force between the disk and the rider specimens.

Materials and Specimen Preparation

Two sets of specimens were used for this study. The disk material was 304 stainless steel (hardness about 260 Vickers hardness number) and the rider material is aluminum oxide. The environmental gas used in this study was chlorine which was 99.5 percent pure.

The rider specimens were acid cleaned before use with aqua regia to remove metal and other contaminants tha might have become embedded in the surface from finishing. They were then rinsed in water, and finally rinsed in ethyl alcohol. Average peak-to-valley roughness in the peripheral direction was about 2 micrometers.

The disk specimen surfaces were finish ground on metallurgical papers to a grit of 600. They were then diamond polished with 6-micrometer and finally 3-micrometer diamond paste. The disks were rinsed with freon and then with absolute ethyl alcohol. The disk specimens were cleaned by ion bombardment by bleeding research-grade argon gas into the system until a pressure of about 0.1 torr was reached. A dc power supply was used to supply 750 volts between

the disk and a floating electrode. The current under this condition was 60 mA. With a negative potential on the disk, positively charged argon ions bombarded and sputter cleaned the specimen surfaces. Sputtering was continued until only peaks for the elements in 304 stainless steel were detected by Auger spectroscopy. The rider surface was covered by a shield of 440C stainless steel to avoid contamination during ion bombardment as indicated in figure 1.

Procedure

Sliding experiments were conducted with the rider specimen loaded against the disk surface in a vacuum of 10^{-6} Pa and 5×10^{-4} Pa of chlorine gas. As the disk was rotated, the rider scribed a circular sliding track on the flat disk surface. The load used in this study was 500 grams, and the rotating speed of the disk specimen was 5 mm/sec. The environmental temperature was 25° C.

Elemental analysis of the disk specimen surface was made before and after the sliding experiments by using an Auger cylindrical-mirror analyzer with an integral electron gun. The beam of the electron gun could be positioned directly into the desired position of the wear contact zone by a sample scanning positioner with a television monitor.

Scanning electron and optical microscope observations were conducted after one pass and after 50 passes sliding of the rider. One pass and 50 passes of sliding were carried out on the same disk specimen surface. Diameters of the sliding tracks were slightly different so as not to overlap each other. The depth of the groove and height of the plateau formed by sliding experiments were determined by adjusting the focus of a lens system on the high magnification optical microscope.

RESULTS

Before conducting sliding experiments, the 304 stainless steel disk surfaces were examined with the Auger spectrometer with the normal oxides and adsorbates on the surface. A typical Auger spectrum is presented in figure 2(a). The elements sulfur, carbon, chlorine, oxygen and iron were detected. The carbon can originate from two sources, (1) absorbed carbon monoxide and/ or carbon dioxide and (2) as an alloying element in stainless steel. The oxygen can result from adsorbates and iron or chromium oxide. Argon ion sputter cleaning of the disk surface resulted in the Auger spectra of figure 2(b) and figure 2(d). Examination of the Auger spectra reveals only peaks for elements of the 304 stainless steel (i.e., Fe, Ni, Cr, C). The surface is free of oxygen, chlorine and sulfur. Based upon these patterns, the disk surface is atomically clean. In figure 2(e), an Auger spectrum is presented for a clean stainless steel surface after being saturated with chlorine by exposure to over 10^5 Langmuirs of chlorine gas. There are, in addition to the peaks of the stainless steel elements, Auger peaks for chlorine.

Two kinds of sliding experiments were conducted: (1) at 10^{-6} Pa with a clean disk and (2) at 5×10^{-4} Pa of chlorine gas with the disk suface that was saturated with chlorine. Examination of figure 2(c) and figure 2(f) indicates essentially no change in Auger peaks after 50 passes over the same surface. An Auger peak for sulfur was slightly detected at the surface after 50 passes under the condition of 10^{-6} Pa. One possible reason is contamination of the rider surface in the process of sputtering. The contaminant seems to transfer to the disk surface during 50 passes of sliding. However, this small amount of contamination has no observable effect on the surface deformation behavior.

Figures 3 shows representative surfaces of the specimens tested at 10^{-6} Pa vacuum and an environment of $5x10^{-4}$ Pa of chlorine gas. Even in the chlorine gas environment, severe shearing and tearing can be observed on the disk surface. Transfer of wear fragments can also be observed on the rider surface under both conditions. Differences observed on the surfaces will be mentioned later using SEM photographs. The initial average value of the friction coefficient was 1.2, but with the establishment of a sliding tract the friction coefficient decreased to a value of 0.5 in the 10^{-6} Pa evironment. Fluctuation of the friction coefficient also gradually decreased with the number of passes. The friction coefficient μ changed from 1.0 to 0.4 at $5x10^{-4}$ Pa of chlorine gas. Again the fluctuation decreased with the number of passes, but the sliding track width was narrower than that observed in a vacuum of 10^{-6} Pa indicating less mean to the rider. This behavior can be explained by the existence of surface films formed in the chlorine gas environment.

Scanning Electron Microscope (SEM) photographs of the deformed surface observed on the sliding wear track after sliding some distance are shown in figure 4. The height and depth of the surface profiles are indicated in the photographs as measures of the distance from the initial level of the disk surface. Two types of characteristic proturberances are observed on the sliding track shown in figure 4(a). One is an isolated island, and the other is represented by intermittently scattered material on the track. The island-shaped protuberances are shown in micrographs of figure 5 under magnification.

Figure 4(b) presents SEM photographs of the deformation observed in the $5x10^{-4}$ Pa chlorine gas environment. The results observed are substantially similar to those observed in a vacuum of 10^{-6} Pa. On all the disk surfaces, characteristic trapezoid-shaped or step-shaped protuberances are formed during

the initial stage of sliding contact. Slip marks are visible on most upper surfaces of the protuberances.

The surface contour of the sliding track observed after 50 passes of the rider is shown in figure 6. Figure 6(a) was obtained in a vacuum of 10^{-6} Pa and figure 6(b) in an environment of 5×10^{-4} Pa chlorine gas. Photographs of the observed sliding tracks obtained by SEM can be compared with those obtained from the optical microscope in figure 7. The non-sliding area and isolated protuberances are observed on the surface after 50 passes of the rider even in the environment of 5×10^{-4} Pa chlorine gas (fig. 7(b)). The protuberances exist in the contacting regions of the sliding surface, not in the unslid portion of the wear track. Results obtained under both the conditions of 10^{-6} Pa vacuum and 5×10^{-4} Pa chlorine gas indicate that the surface layer is gradually torn off and the surface takes on a characteristic geometry.

Examples of wear fragments found on the disk surface are shown in the SEM photographs of figure 8. The left photograph shows examples of large wear fragments found on the surface. A cracked area or flake which will likely be torn off by subsequent sliding can be also observed at the edge of the surface plateau.

A typical topographical representation of a sliding track is illustrated in figure 9(b) which is based on the top photograph. The topography of the sliding track has indications that wear fragments are separated from the edge of surface plateau and that the grooves develop and the plateau becomes smaller.

A summary of the distribution of the height for the surface contour from the figures is presented in figure 10. The distance from the initial height of the disk surface is reflected in the figure. The positive values for one pass sliding represent, of course, the height of protuberances or material

transferred to the sliding track and the negative values denote the depth of the groove located just behind the protuberance. The positive value for 50 passes sliding represents the height of surface plateau and the negative value indicates the depth of the groove located just behind the plateau with respect to the sliding direction. Therefore, for one pass sliding the negative value indicates the depth of the primary shearing which forms the protuberance. The negative value for the 50 pass sliding implies the depth where the detachment which forms a wear fragment occurred.

Wear Process in the Present Study

Characteristic modes of deformation and fracture were observed on the surface of 304 stainless steel disks slid against aluminum oxide riders. The protuberances and slip marks observed on the sliding track, revealed the following predictive mechanism for the formation of the step-shaped protuberances. When surface interactions occur between disk and rider, the surface layer of the disk suffers shearing deformation by the tangential movement of the rider in the sliding process. The surfaces of practical material have a variety of geometric irregularities, unless created by some special techniques such as cleaving. The effective surface roughness is initially large but smaller than the representative radius of curvature in the contact area. This roughness has a tendency to decrease because the transferred material fills in the valleys between asperities. There are, however, many asperities so inclined as to engage each other across the interface in the sliding direction at early stages of the sliding process. Even when the contact changes into the metal-to-metal contact owing to material transfer to the aluminum oxide rider, the interface brought about in this manner is apt to be inclined in a similar way to that indicated by Cocks (ref. 11). In either case, adhesion is

developed preferentially in these areas because the normal component of the sliding force is imposed in the areas.

Since the material involved in the adhesion process suffers plastic deformation, the material existing near the interface is generally work hardened. Furthermore, an interfacial adhesive bond which occurs in the contact zone is generally stronger than the cohesive bond in the cohesively weaker of the two materials. Based on these considerations, the shearing force necessary to separate the interface is usually larger than that of the material located below the interface. Therefore, the surface layer once adhered to the rider surface is sheared at a certain depth below the interface.

Real contact areas incidentally are generally scattered randomly in the apparent contact area. When an infinitesimal part of the surface layer deforms plastically within the real contact area, the deformation cannot extend to infinity in the tangential direction but is concentrated to a limited area. In other words, the deformation must be compensated by the elevation of the localized surface layer. Therefore, the volume of material involved in the contact behavior expands both in the tangential and the vertical directions. The height of partially elevated surface increases gradually in this manner. These phenomena usually occur randomly in the apparent contact area resulting in different size contacts, and furthermore, the rate of development in the vertical direction is generally different for each area. Since the mating aluminum oxide rider has a relatively smooth surface, and valleys of the asperities, will be filled with the transferred material, partial elevations of the disk surface result in vertical movement of the aluminum oxide rider. Therefore, elevated areas will be separated by the vertical movement caused by the elevation at other areas.

The contact area where the specific contact stress exceeds a critical value will be pressed out and flattened on the "parent" surface by the rider during the sliding process. The former process is illustrated schematically in figure 11. The formation of characteristic modes of protuberances and slip marks observed on surfaces (figs. 4 and 5) can be understood better with the use of these mechanisms. More information is needed to fully understand the factors determining the height of the protuberances. The vertical displacement of the rider plays an important role in the formation of the protuberances. Similar phenomena have been reported for different combinations of materials (refs. 5 to 11 and 12).

The disk surface initially smooth will become rougher with repetition of the formation process for the step-shaped protuberances. The protuberances once formed in the initial stage of sliding contact have a chance either to be removed from the surface as a wear fragment or to be pressed on the surface and be flattened. In this manner, the surface layer with a plateau-shaped configuration, probably having a mechanically different properties, will be formed in subsequent sliding processes. The process of wear fragment and sliding track formation can be discussed with a consideration of the contours formed at the sliding surface shown representatively in figure 9.

It is generally difficult for any particle of material to move out of the inside of the plateau as illustrated in figures 12(a), (b), and (c) or from the leading edge of the plateau. On the contrary, if the plateau is shaped like the illustration indicated in figures 12(d) and (e), particles in the surface layer can be taken off more easily from the side edge or the trailing edge of the plateau than from inside the contact area. Therefore, three situations can be modeled and these are shown in figure 13. In all cases, no surface layer exists to oppose the detachment of particles. The shape of the

12

particle is assumed here ideally to be a rectangular parallelepiped. The shear strength of the interface between the rider and the surface layer is represented with τ_0. The shear strenth at the depth of h from the surface is denoted by τ_h. Term σ_t represents the average tensile strenth of the surface layer. The average shear strength of the "side wall" of the area defined by $b \times h$, can be assumed to be approximately $(\tau_0 + \tau_h)/2$. The required critical condition for the balance of forces allowing the detachment of a particle can be described as follows.

Case (a): Detachment from the corner of plateau

$$\tau_0 ab > \sigma_t ah + \tau_h ab + \frac{\tau_0 + \tau_h}{2} bh \tag{1}$$

$$(\tau_0 - \tau_h)a - (\tau_0 + \tau_h)\frac{h}{2}b > \sigma_t Ah \tag{2}$$

The left term must be positive to have a physical meaning. Then,

$$(\tau_0 - \tau_h)a > (\tau_0 + \tau_h)\frac{h}{2} \tag{3}$$

Again for equation (3) to have physical meaning,

$$\tau_0 > \tau_h \tag{4}$$

Therefore, the requirement of (3) is reduced to

$$a > \frac{\tau_0 + \tau_h}{\tau_0 - \tau_h} \cdot \frac{h}{2} \tag{5}$$

and the requirement (1) is reduced to

$$b > \frac{\sigma}{(\tau_0 - \tau_h)a - (\tau_0 + \tau_h)\frac{h}{2}} ah \tag{6}$$

Case (b): Detachment from the trailing edge of strip-shaped plateau

The required condition here becomes more simple.

$$\tau_0 ab > \sigma_t ah + \tau_h ab \tag{7}$$

$$(\tau_0 - \tau_h)b > \sigma_t h \tag{8}$$

For the equation to have a physical meaning, the same equation as (3) must be valid. Then the equation for (7) becomes

$$b > \frac{\sigma_t}{\tau_0 - \tau_h} h \tag{9}$$

Case (c): Detachment from the trailing edge inside plateau

The equation for the balance of forces which can cause the detachment of the particle is described as follows:

$$\tau_0 ab > \sigma_t ah + \tau_h ab + \frac{\tau_0 + \tau_h}{2} 2bh \tag{10}$$

$$(\tau_0 - \tau_h)a - (\tau_0 + \tau_h)h \quad b > \sigma_t ah \tag{11}$$

For equation (11) to have a physical meaning, the left term of equation (11) must be positive

$$(\tau_0 - \tau_h)a > (\tau_0 + \tau_h)h \tag{12}$$

Again, if assumption (4) is valid, equations (11) and (12) are reduced to the following equations, respectively:

14

$$a > \frac{\tau_0 + \tau_h}{\tau_0 - \tau_h} h \qquad (13)$$

$$b > \frac{\sigma_t}{(\tau_0 - \tau_h)a - (\tau_0 + \tau_h)h} ah \qquad (14)$$

As indicated above, the most fundamental equation assumed here is (4). The strength of the 304 stainless steel disk is weaker than the aluminum oxide rider. An interfacial adhesion bond develops in the contact area, is generally stronger than the cohesive bond in the cohesively weaker of the two materials that of stainless steel. The detachment should therefore occur in a 304 stainless steel disk. Then, the assumption of equation (4) is not in contradiction to the foregoing phenomena.

Taking into account the schematic geometries of figures 12(d) and (e), and the principal models of figure 13 initial configurations should have a tendency to change gradually into the final stable profile being more parallel with respect to the sliding direction, as shown in figure 14. The contour of sliding track corresponds with that shown in figure 9. On the other hand, in the steady state, particles are torn away from the plateau, and the area located within a groove which has been formed in the process of removing the plateau begins to participate in the contact process forming partially an element of a new plateau and partically step-shaped protuberances. It should be noted that a particle which is detached from the plateau does not necessarily become a wear fragment. A detached particle will probably be crushed into smaller pieces, and in some cases small fragments adhere to each other between the contacting surfaces to develop into a wear fragment.

DISCUSSION

There is a view that wear fragments should be produced as a fatigue process through repetitive loading which will be applied either in the process of one pass or multipass sliding on a mating surface. In the former, the repetition is assumed to be realized by the multi-interactions of the surface asperities within the contact area. The essence of fatigue is the phenomenon that the microcrack initiated in the material can propagate only under the condition of repetitive loading and cannot develop under static loading of the same magnitude. When the concept of fatigue is adapted to wear, a more exact comparison must be made based on reasonable mechanics.

The phenomena of crack growth in fatigue should be of course related to the separation of the surface layer in some depth in the parent material during the wear process. Metal transfer which implies the separation of surface layers can take place during one pass of the rider, as well as multipass sliding. Metal transfer can be observed at the instance of a single contact and sliding. In other words, the separation and fracture can always occur in the material without the aid of repetitive loading at the contact surface. Therefore, the most essential element of the wear process in the unlubricated condition is not introducing the concept of repetitive loading (i.e., fatigue) but rather presenting a reasonable explanation as to how the interface can be separated again during sliding based on the concept of adhesion.

Investigators who emphasize the concept of fatigue pay much attention to the behavior of material properties which change with the number of repetitive passes of sliding. This viewpoint is frequently applied to the wear process for the moderate sliding contact where the material transfer does not prevail. Some material property may change and deteriorate into the situation which facilitates the crack formation leading to wear fragment formation.

Fracture criterion is generally determined from the material properties and stresses involved in the fracture process based on a knowledge of fracture mechanisms. Therefore, if the assumption is made that material deterioration makes the fracture criterion shift down for crack initiation or propagation by loading, variation of material properties can be treated with and included in the mechanical conditions. This can be done independently of applying the concept of fatigue.

The present authors' opinion as to how the interaction can be treated based on the concept of adhesion during sliding should be described as follows:

In the contact process with extremely light loads, a certain amount of elastic strain energy is stored in the material located near the interface. The elastic strain energy is produced through the relative micro displacement occurring at the interface and the plastic deformation in the interacting area. This is especially true in such a mechanical process as sliding, where displacement accompanied by the plastic deformation occurs at the surface both in the normal and the tangential directions. The order of elastic strain at the elastic limit does not usually exceed 10^{-2} Pa for ordinary metals. Assuming the representative length of real contact area relative to adhesion to be 10 μm, the absolute displacement corresponding to the strain of 10^{-2} Pa is 10Å. The occurrence of displacement fluctuations of the order 10Å is mechanically not avoidable either in the tangential or normal direction even when the sliding conditions are controlled carefully. With the relatively soft material, annealed aluminum or copper for example, the elastic strain energy stored in the material will be released easily by the subsequent plastic deformation process.

What kind of mechanism can be assumed to occur for metals other than soft ones. The real contact area generally consists of each of the contacting "spots" Ar_1, Ar_2, etc. in contact, as shown in figure 15(a). There are a variety of binding situations in the real contact area owing to the character of interactions. For example, interposing the environmental gas molecule and mismatching in the metal structure. Therefore, the tribological concept of the real contacting area is illustrated in figure 15(b). The binding force in the interfacial surface may be distributed as shown in figure 15(c). If a shearing force is applied to the real contact area, the cohesively weaker region may be detached. When the spot involved in the bonding escapes from the environment pressurized by the interaction, the interface is separated partially at the area bonded more weakly with the aid of the release of elastic strain energy. The separated area include fractures at the extremely sharp-edged pre-existing cracks which generally cause the large stress concentration at the interface. Therefore, the average shearing force required for detaching the specific "apparent real" contact area decreases markedly. This latter force may be less than that in the interior bonding of the same magnitude. In other words, the average shearing force required for separating the specific real contact area at the tribological surface can be greater than that of cohesively weaker material only under the condition that the interface is pressurized by the normal component of external loading. Even if the fracture occurs below the interface, its location should be close to the interface because the real contact area is predicted to be very small at this stage.

As described previously, the rider inevitably moves up and down in the sliding process. Therefore, the interface of some spot can be separated in the process of upward movement without the aid of the tangential force. This behavior facilitates the aforementioned separation mechanism at the inter-

face. The following characteristics for the separation behavior should be noted. Protuberances can develop partially by shearing as a result of the tangential movement of the rider which takes place below the interface. As observed on the surface in the one pass sliding process, the surface layer partially accumulated and developed is detached after the rider slides some distance. This is not in contradiction with the strength properties observed in the relationship between the interface and the cohesively weaker material. Several protuberances are generally produced at the contact area, the growth rates of which are different from each other. Therefore, the detachment occurs at or near the interface of one protuberance with the aid of the upward movement of the rider surface which is caused by the protuberances developed at other locations. The tendency is also not in contradiction to the separation mechanism already described.

As already indicated, repetitive loading is not the only mechanical factor causing surface layer fracture in the sliding process where metal transfer occurs. Therefore, the application of fatigue must be limited to certain situations, for example, where (1) sufficient magnitude of tangential force cannot be expected to occur, (2) constraint is unavoidable at the surface in the normal direction or (3) the relative displacement is comparatively small in the tangential direction between contacting surfaces. An example for the former (1) is a wear process where the surfaces are sufficiently lubricated. Ordinary rolling contact fatigue observed under the condition of small roll/slip ratios and fretting are typical examples for the latter (2), (3). In these latter situations, the term "fatigue" has been used adequately and the mechanism described in this study does not apply.

CONCLUSIONS

The deformation and wear process brought about at 304 stainless steel disk surfaces slid against aluminum oxide riders were observed using a scanning electron and an optical microscope. Experimental results are discussed on the basis of adhesion. Boundary conditions to which a realistic wear mechanism should be subject and to which fundamental information on adhesion can be applicable are discussed.

If the material removal process is simplified by assuming it to be based on the adhesion theory, the mechanism for tearing away of the surface layer from the contact area and the sliding track contour can be explained. The principal results obtained from the experiment are as follows:

1. The surface layer of the disk accumulates and is developed successively behind the rider. Step-shaped protuberances are set up in the initial steps of sliding contact even under a chlorine gas environment.

2. The primary shearing which forms the protuberance occurs in an extremely shallow region of 1 μm located below the contact surface.

3. The "junction growth" occurs inevitably in the vertical direction between the contact surface which is an essential factor in producing the protuberances.

4. A matured surface layer develops at the contact surface and is predicted to be gradually torn off taking a characteristic morphological contour in the sliding track.

5. The material separation producing wear fragments occurs at the depth of 2 to 3 μm.

REFERENCES

1. Graham, D. and Baul, R. M.: An Investigation into the Mode of Metal Removed in the Grinding Process, Wear, 9, pp. 301-314 (1972).

2. Sakamoto, T. and Tsukizoe, T.: Friction and Prow Formation in a Scratch
   Process of Copper by a Diamond Cone, Wear, 44, pp. 393-403 (1977).

3. Barquins, M., Kennel, M. and Courtel, R.: Comportement de Monocristaux de
   Cuivre sous L'Action de Contact d'un Frotteur Hemispherique, Wear, 44, pp.
   393-403 (1977).

4. Kayaba, T., Kato, L. and Nagasawa, Y.: Abrasive Wear in Stick-Slip Mo-
   tion, Wear of Materials 1981, ASME, pp. 439-446 (1981).

5. Landheer, D. and Zaat, J. H.: The Mechanism of Metal Transfer in Slid-
   ing Friction, Wear, 27, pp. 129-145 (1974).

6. Antler, M.: Wear, Friction and Electrical Noise Phenomena in Severe
   Sliding Systems, ASLE Trans., 5, pp. 297-307 (1962).

7. Cocks, M.: Interaction of Sliding Metal Surfaces, Journal of Applied
   Physics, 33, pp. 2152-2161 (1962).

8. Antler, M.: Process of Metal Transfer and Wear, Wear, 7, pp. 181-203
   (1964).

9. Cocks, M.: Role of Displaced Metal in the Sliding of Flat Metal Sur-
   faces, Journal of Applied Physics, 35 pp. 1807-1814 (1964).

10. Cocks, M.: The Formation of Wedges of Displaced Metal Between Sliding
    Metal Surfaces, Wear, 8, pp. 85-92 (1965).

11. Cocks, M.: Shearing of Junction Between Metal Surfaces, Wear, 9, pp.
    320-328 (1966).

12. Sasada, T., Norose, S. and Mishina, H.: The Behavior of Adhered Frag-
    ments Interposed Between Sliding Surfaces and the Formation Process of
    Wear Particles, ASME Trans., 103, pp. 195-202 (1981).

13. Buckley, D. H.: Surface Effects in Adhesion Friction, Wear and Lubrica-
    tion, Elsevier, Chap. 5 (pp. 245-313) (1981).

CD-81-12631
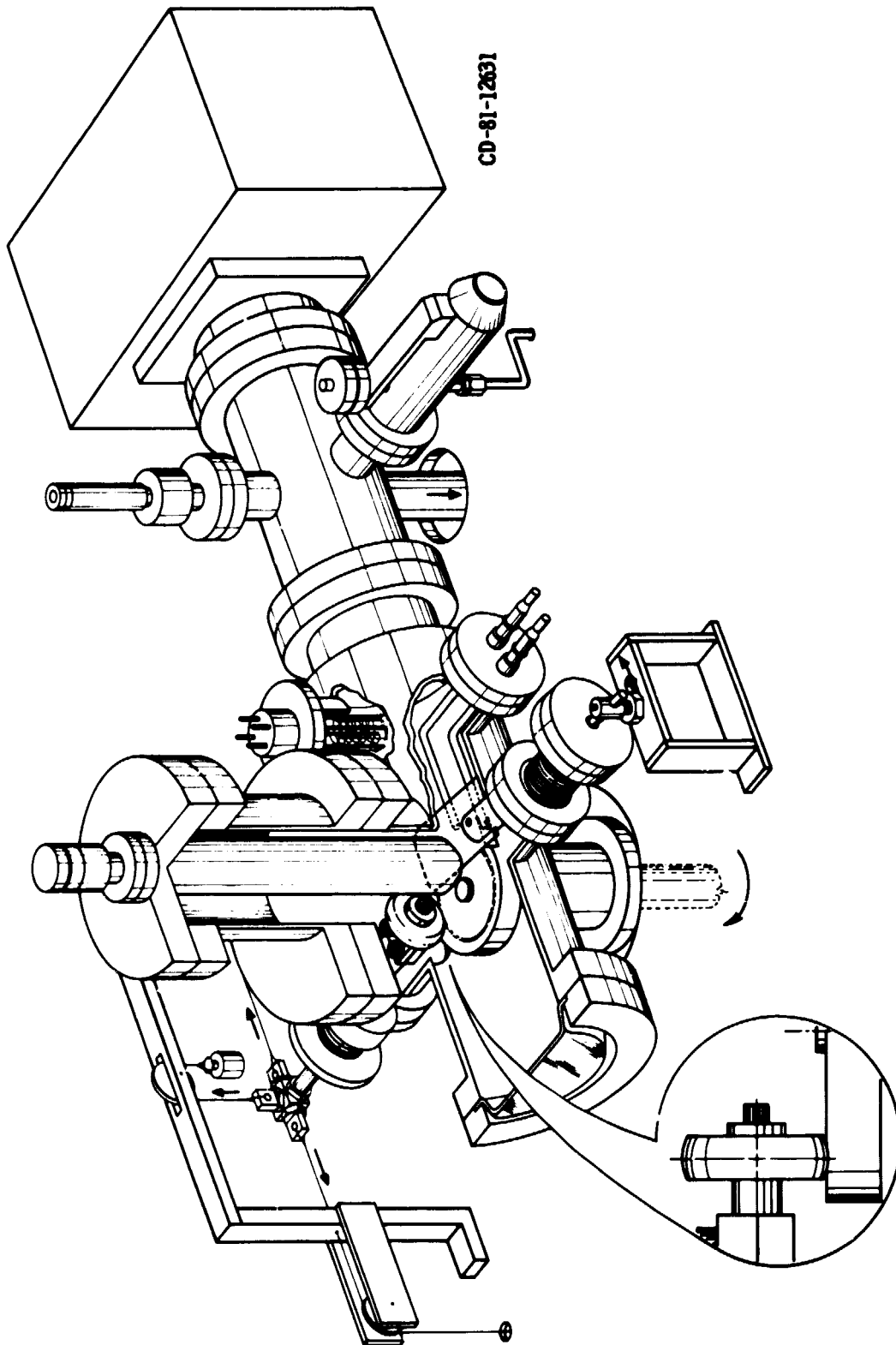
Figure 1. - Sliding and rolling contact apparatus with auger spectrometer.

(a) Specimen used for 10^{-8} torr vacuum before sputter cleaning.

(b) Specimen used for 10^{-8} torr vacuum after sputter cleaning.

(c) Specimen used for 10^{-8} torr vacuum after 50 passes.

(d) Specimen used for 5×10^{-6} Cl gas environment after sputter cleaning at 10^{-8} torr vacuum.

(e) Specimen used for 5×10^{-6} Cl gas environment after exposed in chlorine gas environment.

(f) Specimen used for 5×10^{-6} Cl gas environment after 50 passes.
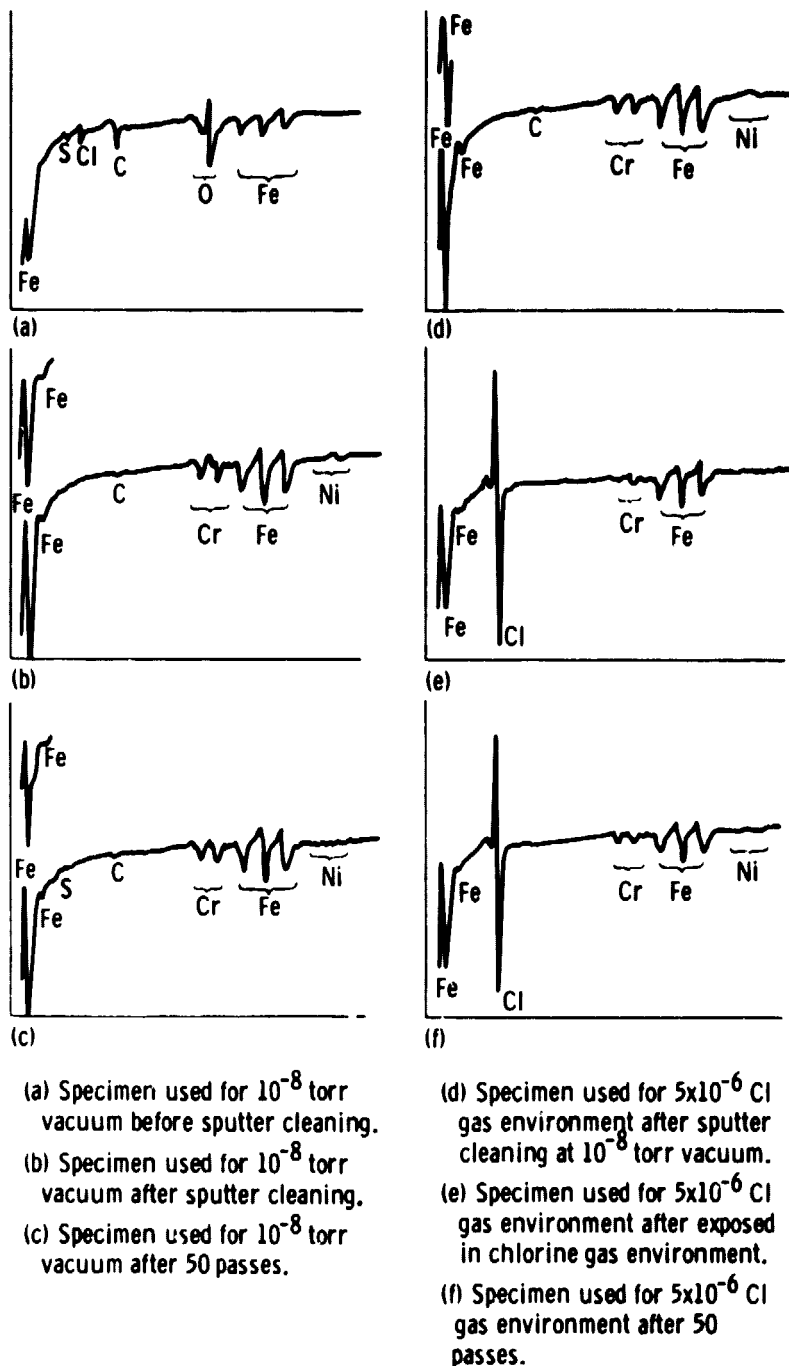
Figure 2. - Auger spectra for 304 stainless steel disk surface.

10^{-8} TORR VACUUM

5X10^{-6} TORR CHLORINE GAS ENVIRONMENT

SLIDING DIRECTION

X200

X1000
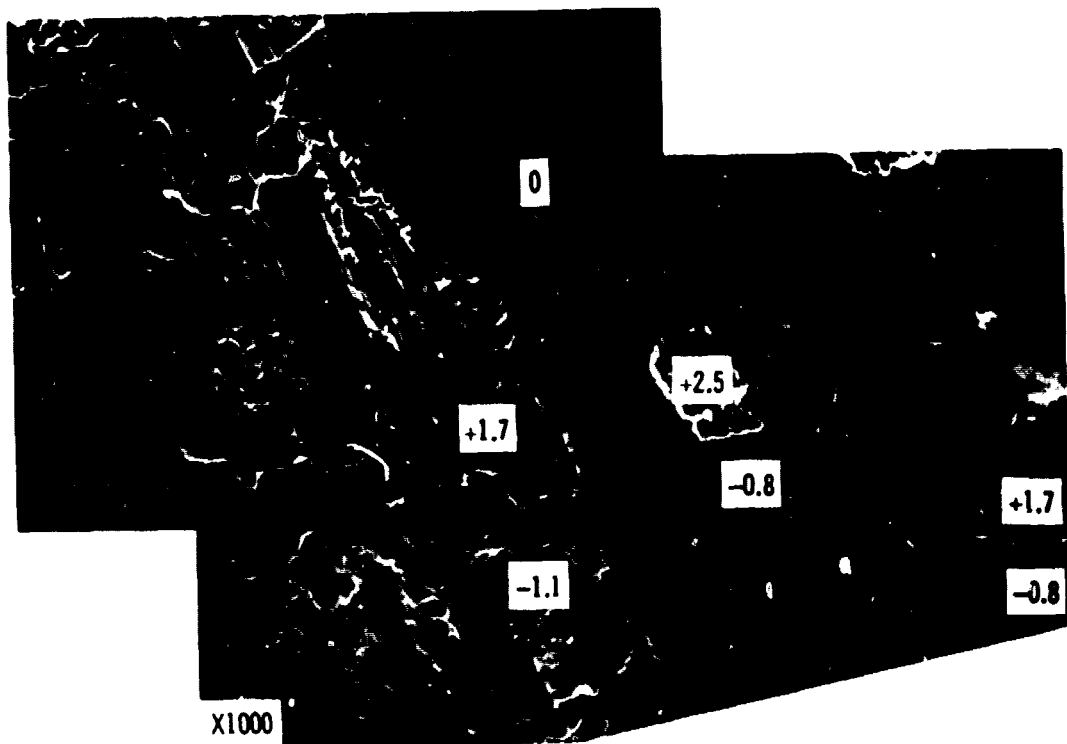
(a) 10^{-8} Torr vacuum.

Figure 4. - Plastic deformation on disk surface after one pass.
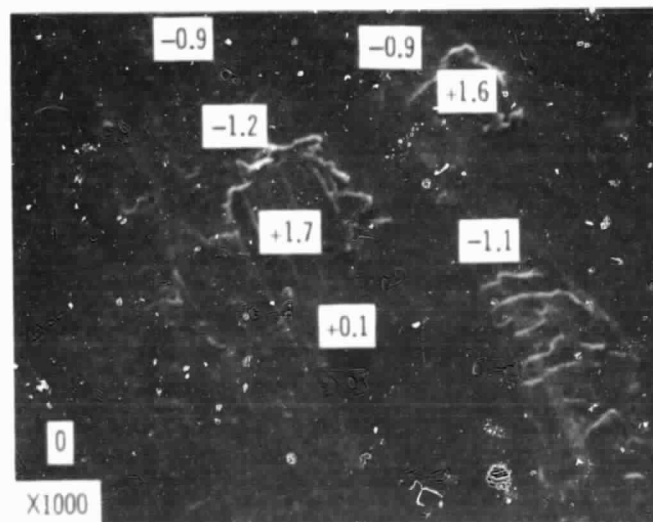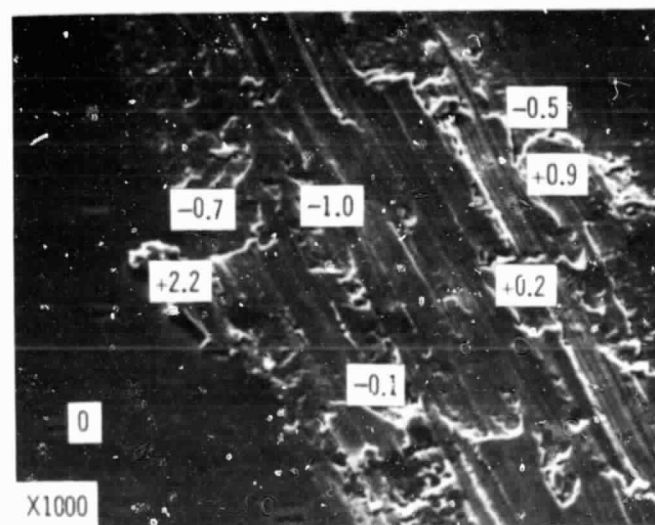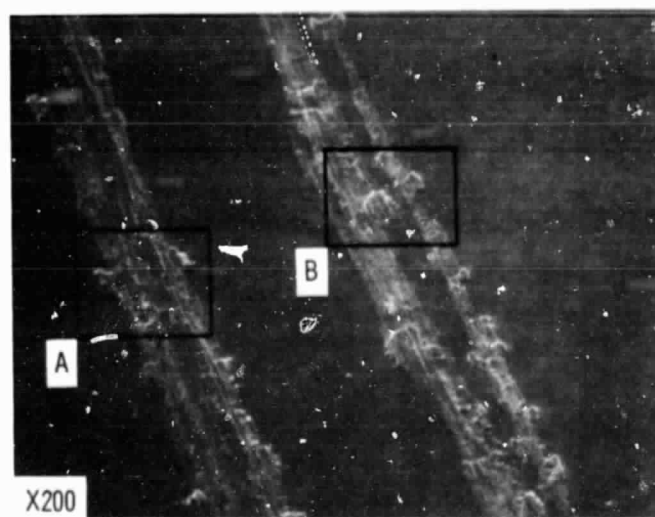
(b) 5X10^{-6} Torr chlorine gas environment.

Figure 4. - Concluded.

X5000

X1000

SLIDING DIRECTION
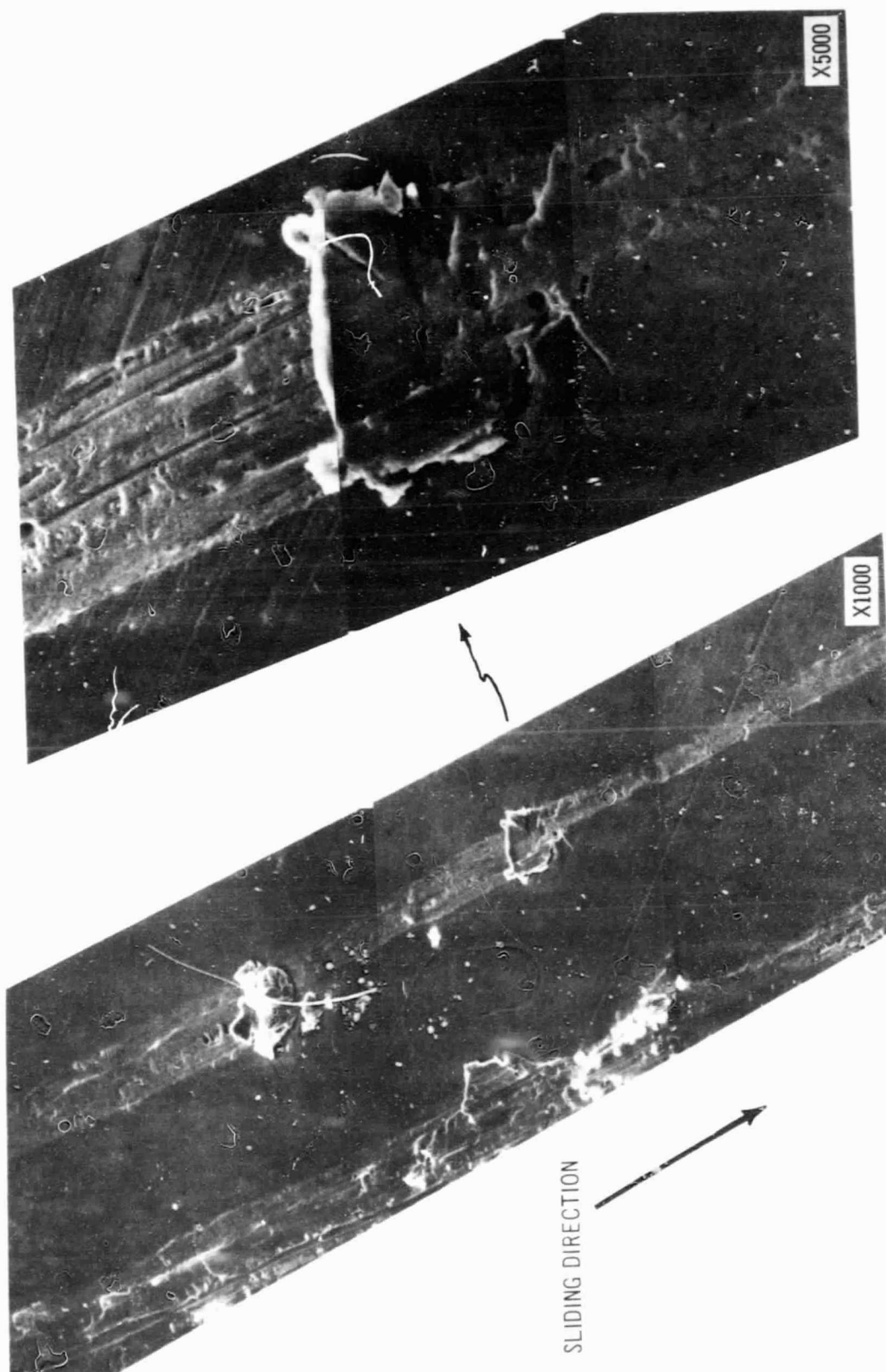
Figure 5. - Typical isolated mode of protuberances, one pass, 10^{-8} torr vacuum.
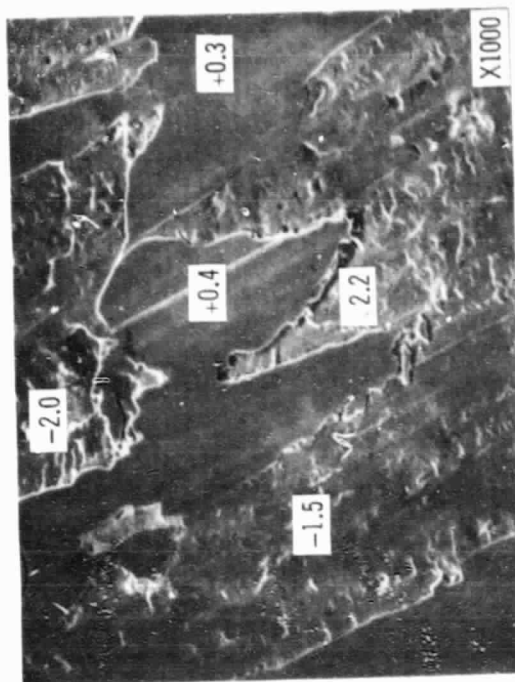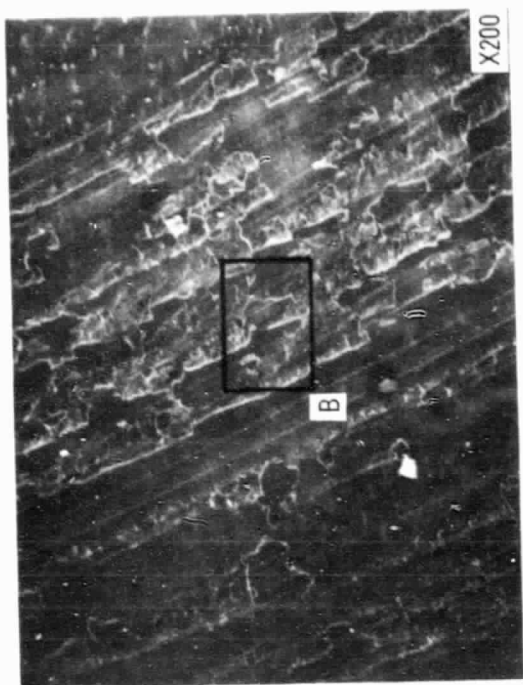
(b) 5X10⁻⁶ Chlorine gas environment.

(a) 10⁻⁸ Torr vacuum.

Figure 6. - Plastic deformation on disk surface after 50 passes.
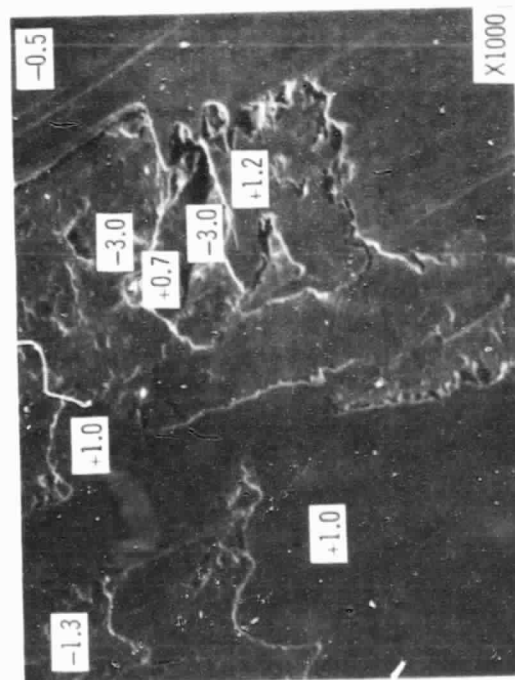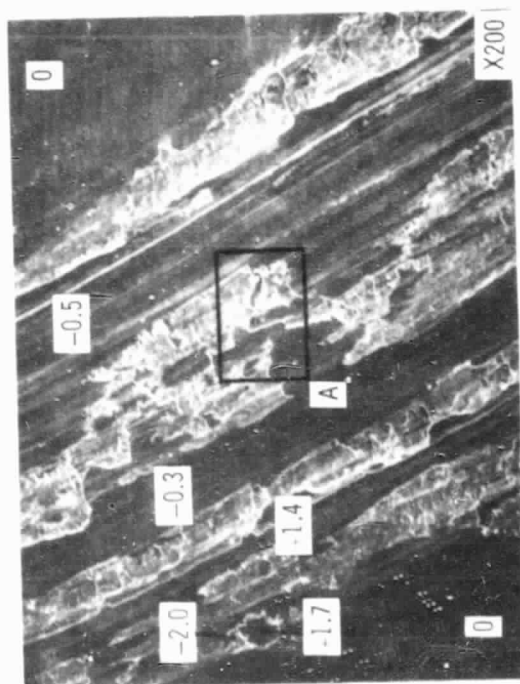
(SEM)

(OPTICAL MICROSCOPE)

SLIDING DIRECTION

(a) 10⁻⁸ Torr vacuum.

(b) 5X10⁻⁶ Torr chlorine gas environment.

Figure 7. - Comparison of sliding track on disk surface after 50 passes.

X1000

(b) 5X10^{-6} Torr chlorine gas environment.

X1000
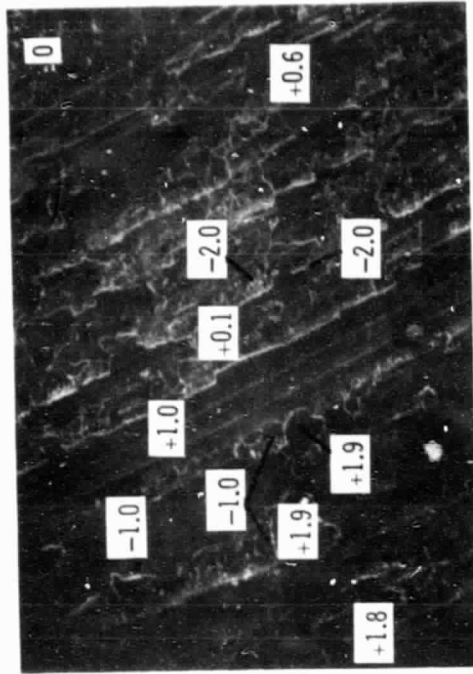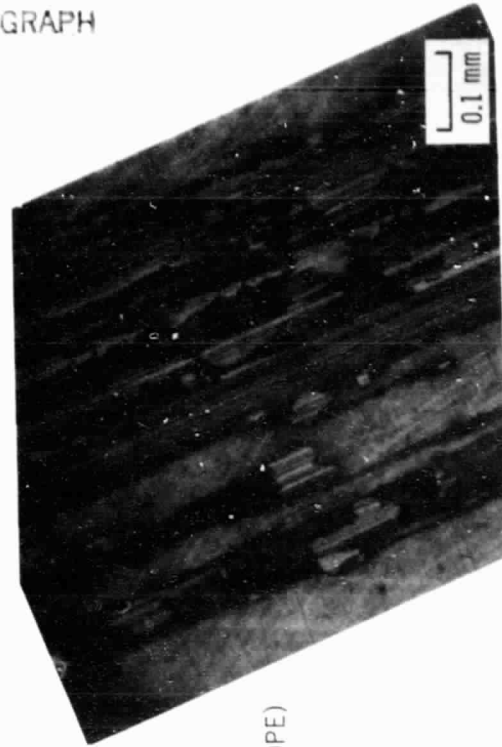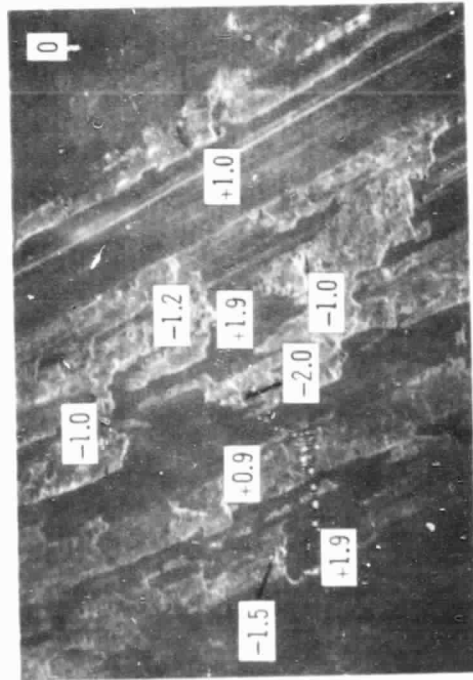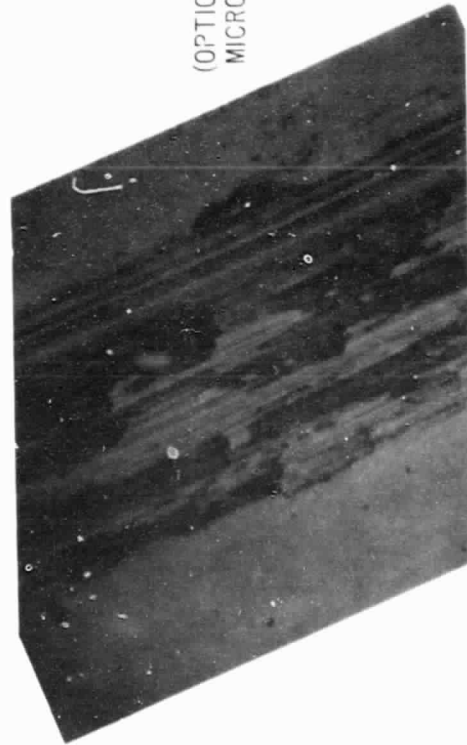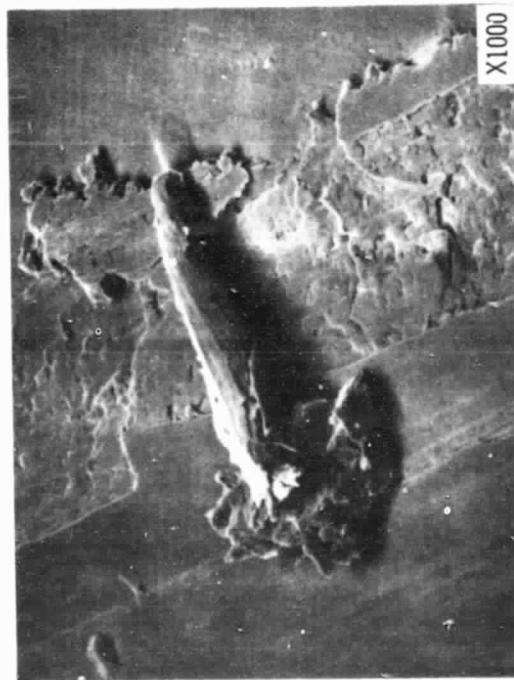
(a) 10^{-8} Torr vacuum.

SLIDING DIRECTION

Figure 8. - Examples of wear fragment observed in the sliding track of disk after 50 passes.
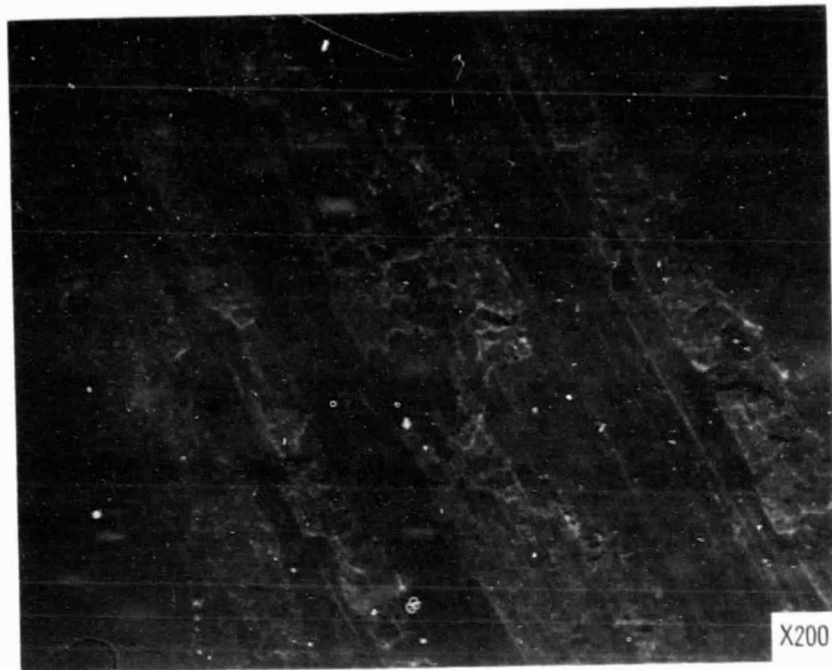
(a) Typical sliding track.
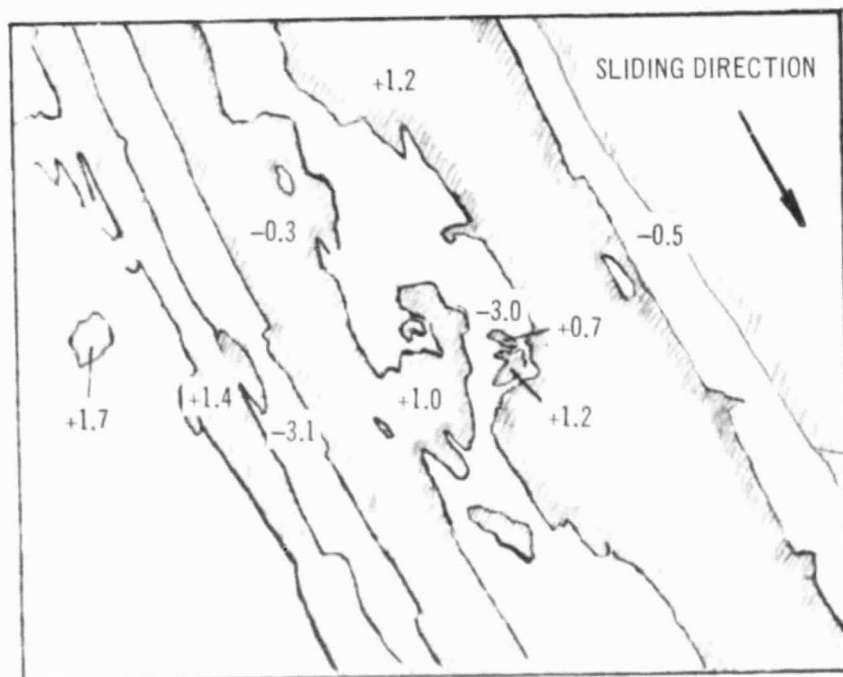
(b) Topographical representation of sliding track.

Figure 9. - A typical contour of sliding track.

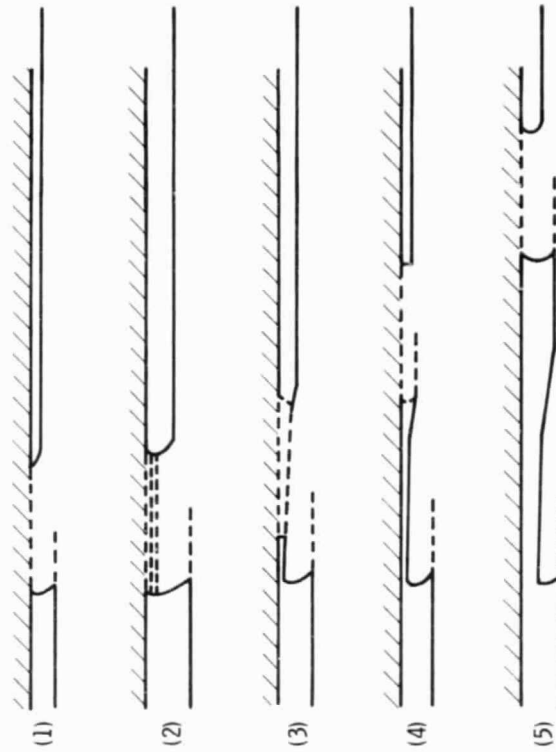(1) - (2) Accumulation process
(3) - (4) Separation process
(4) - (5) Accumulation process

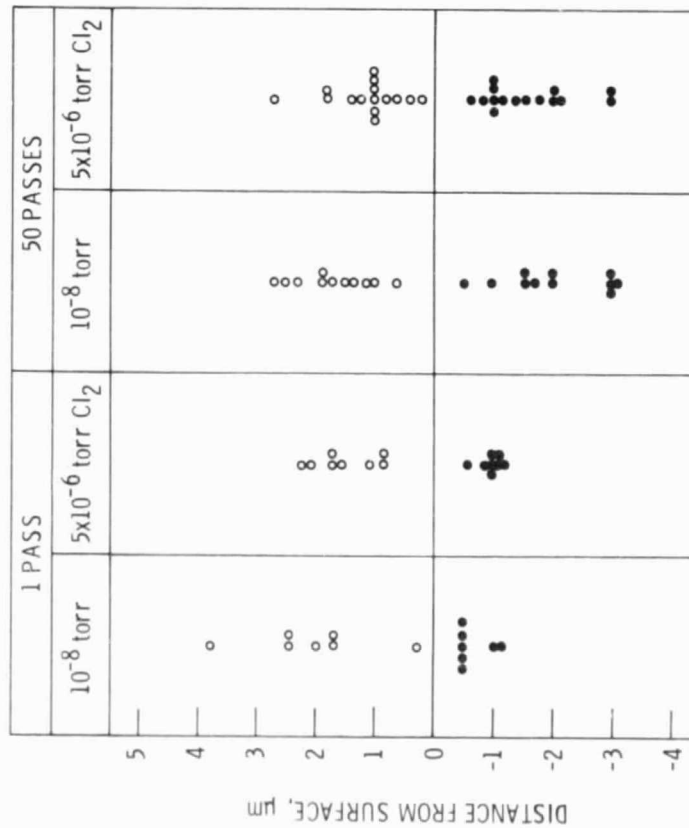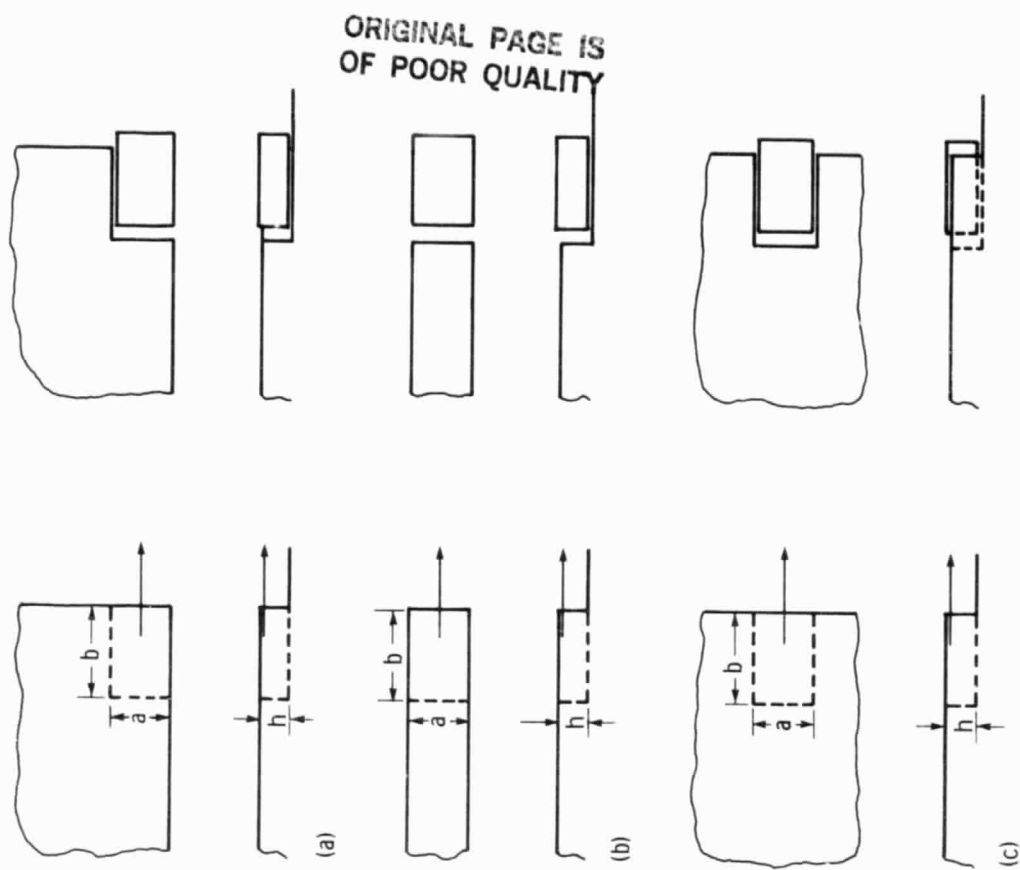Figure 11. - Process for the formation of protuberances in this study (ref. 10).
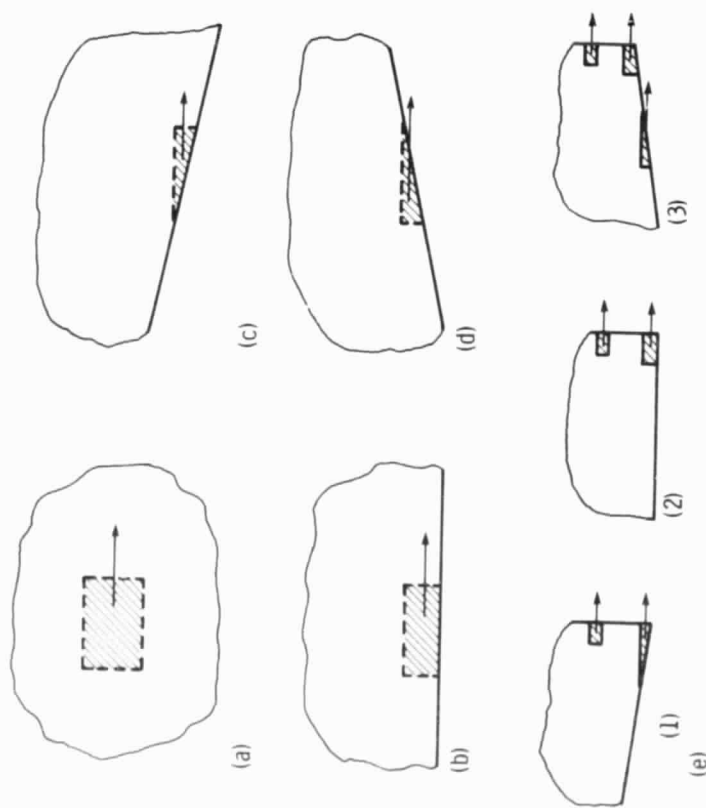

Figure 10. - Height of protuberances and depth of grooves formed in sliding track.

(a) Detachment from the corner of plateau.
(b) Detachment from the trailing edge of strip-shaped plateau.
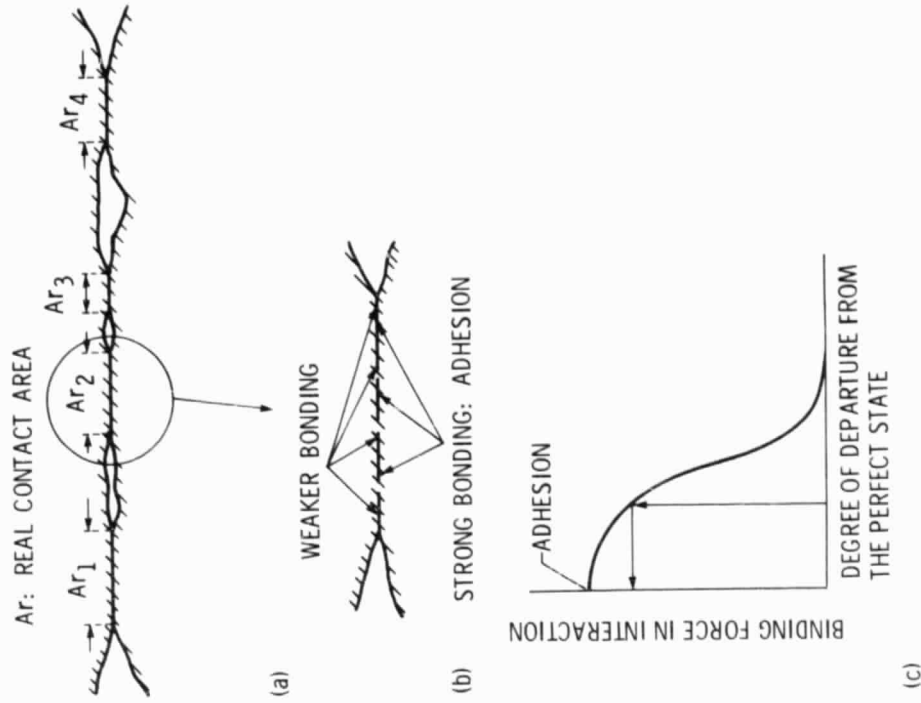(c) Detachment from the trailing edge inside plateau.

Figure 13. – Three models for detachment of particles from a plateau.

(a) – (c) Contours where lumps are not easily removed.
(d), (e) Contours where lumps are easily removed.

Figure 12. – Illustrations of various contours on sliding track where particles
from the surface layer are removed.

Ar: REAL CONTACT AREA

Ar_1 Ar_2 Ar_3 Ar_4

(a)

WEAKER BONDING

STRONG BONDING: ADHESION

(b)

ADHESION

BINDING FORCE IN INTERACTION

DEGREE OF DEPARTURE FROM
THE PERFECT STATE

(c)

(a) Schematics of real contact area.
(b) Schematics of real contact area.
(c) Concept of binding force in real contact area.

Figure 15. - Concept of real contact area.

INITIAL → FINAL

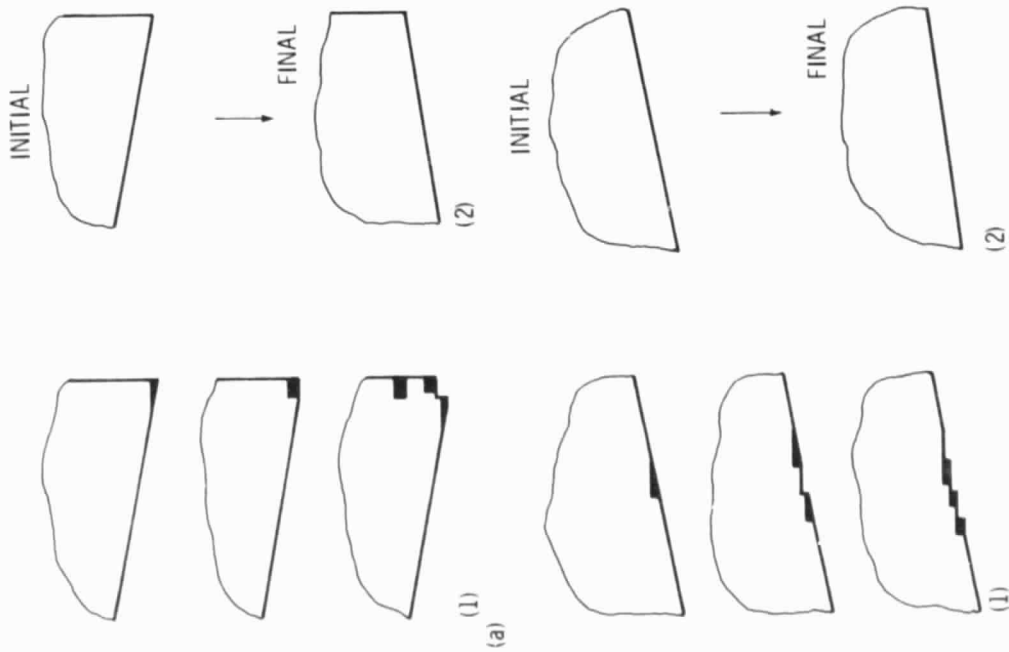(2)

INITIAL → FINAL

(2)

(1)

(a)

(1)

(b)

Figure 14. - Two types of transformation of initial contours
into stable ones on sliding tracks.